Analysis of Complex X-ray Amorphous Phase Assemblages with Potential Applications as Martian Soil Simulants. A. Pandey[1], P. Schwab[2], Y. Deng[2], D. W. Ming[3], E. B. Rampe[3], S. A. Mertzman[4]. [1]Texas A&M University (pandeyaditi@tamu.edu), [2]Texas A&M University, [3]NASA JSC, [4]Franklin and Marshall College.

Introduction: The Chemistry and Mineralogy (CheMin) X-ray diffraction (XRD) instrument onboard the Mars Science Laboratory Curiosity rover has revealed between 15 to 75% (w/w) X-ray amorphous materials suspected to be ferrihydrite, nanophase hematite, opaline silica, silicate glass, and/or allophane in ancient sedimentary rocks and modern aeolian sediments in Gale crater [1,2,3,4,5]. Short range order, chemical heterogeneity, and complex bonding assemblages in naturally occurring amorphous minerals increase the error associated in quantifying such phases. This study proposes a robust laboratory-scale approach for quantifying chemical composition of amorphous phase in mixed samples. It compares abundances determined from chemical extractions based on differences in dissolution rates between phases with results from X-ray spectroscopy-based mass balance calculations.

Five samples (HWMK 155R, VC, 101, 153R, and 852), with X-ray diffraction analysis showing no detectable phyllosilicates and at least 20% (w/w) X-ray amorphous materials, were collected from an archive of volcanic soil samples at the NASA Johnson Space Center in Houston, Texas. They were sampled from a 6 km radius around Hawaii's Mauna Kea summit between the elevations of 2010 and 3730 m.

Amorphous Chemical Composition: X-ray spectroscopic and chemical extraction analyses were conducted using 250 µm fraction subsamples, and the results from two samples are summarized in Table 1. Half unit cell formulae of plagioclase feldspar, pyroxene, and olivine were calculated by correlating refined unit-cell parameters with experimentally determined stoichiometries using the algorithm and database of Morrison et al. [6]. Remaining concentrations after subtracting chemical contributions of the crystalline phases (XRD) from the total chemistry (XRF) were assigned to the amorphous phase (Table 1).

A 2 *M* sodium carbonate (Na_2CO_3) solution was used to extract silicates in a constantly stirred batch reactor system maintained at 85°C. A fixed aliquot of solution was collected every over time and concentration of Si as percent mass of the sample was determined via a modified molybdate-blue colorimetric method [7] (Fig. 1). Amorphous contribution of the observed %Si was calculated by fitting concentrations to a linear model assuming an amorphous and crystalline (overall) Si source in the sample, $Si_{aq} = [Si_{extr}](1 - e^{-kt}) + bt$, where [$Si_{extr}$] is the extractable Si from the amorphous phase *i*, k_i the reactivity constant of *i*, and b is the slope of the linear dissolution reaction for the crystalline phase [8].

A similar approach was taken to extract poorly crystalline Al oxides, allophane, imogolite, and X-ray amorphous Fe using Tamm's reagent (0.1 M ammonium oxalate and oxalic acid solution) at pH 3 without light (Fig. 2).

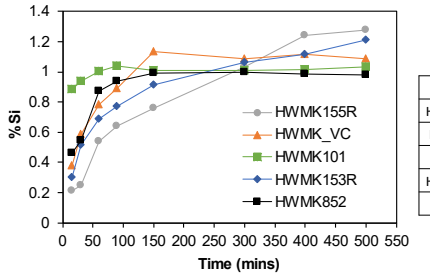

Samples	%Amp Si
HWMK155R	0.792
HWMK_VC	1.056
HWMK101	0.968
HWMK153R	0.552
HWMK852	0.973

Fig. 2*. Percent Si in the 2M sodium carbonate extraction solution with time. Concentrations in amorphous phase calculated from regression analysis using a kinetic model are listed.*

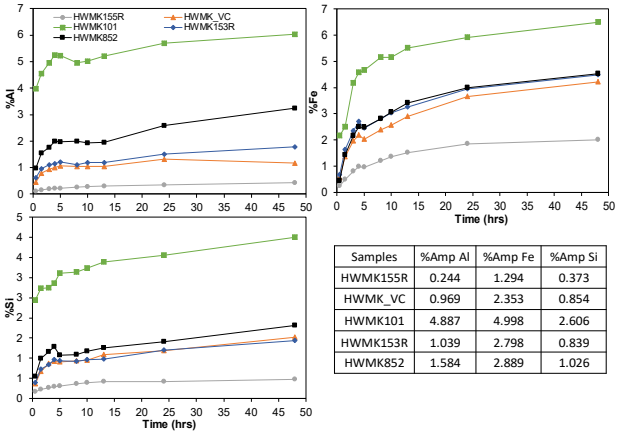

Samples	%Amp Al	%Amp Fe	%Amp Si
HWMK155R	0.244	1.294	0.373
HWMK_VC	0.969	2.353	0.854
HWMK101	4.887	4.998	2.606
HWMK153R	1.039	2.798	0.839
HWMK852	1.584	2.889	1.026

Fig. 1. *Percent Al, Fe, and Si in the ammonium oxalate oxalic acid extraction solution over time. Concentrations in amorphous phase calculated from regression analysis using a kinetic model are listed.*

Proof of Concept: Standard diatomaceous sample was tested with the modified 2 *M* Na_2CO_3 extraction method and imaged to verify the completion of the extraction (Fig. 3). By the end of 500 min., diatom structures were not observed in the SEM micrograph (Fig 3a, 3b). A range of standard reference materials will be used to test the validity of the procedure and the selectivity for amorphous phases**.**

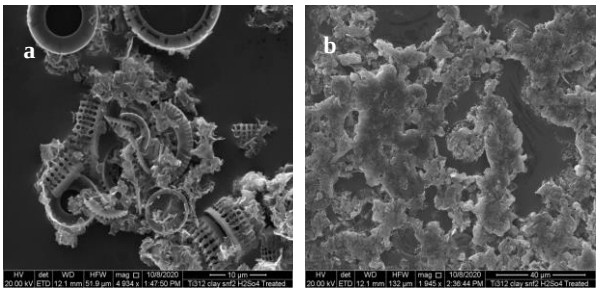

Fig. 3*. Standard diatomaceous sample a) ordered diatoms before extraction, and b) 500 minutes after extraction with 2 M Na_2CO_3. The residual mass in (b) is residual aluminosilicates.*

Table 1*. Amorphous composition calculated from mass balance of QXRD and XRF mineral and chemical concentrations and results from chemical extraction. Unit cell formulae: andesine $(Na_{0.48},Ca_{0.52})Al_{1.48}Si_{2.52}O_8$; augite $(Mg_{1.07},Ca_{0.94})Si_2O_6$; o-pyrexene $Mg_2Si_2O_6$; olivine $(Mg_{1.3}Fe_{0.7})SiO_4$; hematite Fe_2O_3.*

XRF		Andesine	Augite	o-Pyroxene	Olivine	Hematite	Amorph. (Mass Balance)	Amorph. (Chem. Extr.)
	---------- % of total mass (w/w) ----------							
Si	20.0	12.5	1.8	0.7	1.3		*3.8*	3.6
Al	12.7	7.0					*5.7*	4.9
Fe	10.8				1.8	0.9	*8.5*	8.6
Ti	2.1						*2.1*	
Mn	0.2						*0.2*	
Mg	2.0		1.0	0.6	1.4		*-0.9*	
Ca	3.4	3.4	0.9				*-0.8*	
Na	2.2	2.1					*0.1*	
K	0.7						*0.8*	
P	0.5						*0.6*	
O	45.8	22.5	5.5	1.1	2.9	0.4	*12.3*	
						Total →	*34.0*	
XRD Total		47.6	7.0	2.4	7.2	1.3	34.5	

Mass Balance Calculation: The first eight columns of Table 1 contribute to the mass balance calculation, and the final column lists the results from all the chemical extractions. The first two columns list the total elemental composition (%) as determined by XRF. Weight fractions of the crystalline minerals calculated from QXRD are listed in the last row. Based on the estimated half unit cell formula and weight fraction of each minerals, the elemental mass fraction contributing to the mineral is removed from the total. Assuming that the crystalline mineral phases are limited to those identified using XRD, we can subtract the percent of elements contributed from crystalline sources and deduce the elemental composition of the amorphous phase as given in column eight of Table 1. The Si, Al, and Fe concentrations in the amorphous phase from mass balance calculations compare well to concentrations from chemical extraction (final column), improving our overall confidence in both analytical methods. Initial calculations yielded an over-assignment of Mg and Ca, resulting in a negative composition. This is likely the result of simplification of the unit cell formulae for pyroxenes and feldspars: Ti^{2+} and Mn^{2+} are excluded from the unit cells, and Mg, Na and Ca are over-assigned. This hypothesis was supported by the EDS analysis of a plagioclase feldspar that showed the presence of Ti, Na, Mg, and Fe in this phase. Transmission images, elemental mapping, and information on bonding environment from a high resolution of a synchrotron STXM coupled with NEXAFS will provide better structural models to interpret mechanisms of mineral alterations in similar basaltic samples.

References: [1] Rampe E. B. et al. (2020) *Geochem. J., 80,* 125605. [2] Bishop J. and Murad E. (2002) *Am Min, 20,* 357–370. [3] Treiman A. H. (2016) *J. Geophys. Res. Planets, 121,* 75–106. [4] Morris R. et al. (2001) *J. Geophys. Res. Planets, 106,* 5057-5083. [5] Smith R. J. et al. (2018) *J. Geophys. Res. Planets, 123,* 2485-2505. [6] Morrison S. M. et. al. (2018), *Am. Min., 103,* 857-871. [7] Mortlock R. A. and Froekich P. N. (1989) *Soil. Res. 57,* 1-16. [8] Koning E. et al. (2002) *Aquat. Geochem. 8,* 37-67.